ORIGINAL ARTICLE
DOI: https://doi.org/10.30932/1992-3252-2022-20-4-2

World of Transport and Transportation, 2022,
Vol. 20, Iss. 4 (101), pp. 163–172

Optimisation of the Aerodynamic Shape of a Monorail Suspended Unibus

Anatoli E. UNITSKY

Sergey V. ARTYUSHEVSKY

Mikhail I. TSYRLIN

Anatoli E. Unitsky [1], ***Sergey V. Artyushevsky*** [2], ***Mikhail I. Tsyrlin*** [3]
[1, 2, 3] *String Technologies CJSC, Minsk, Belarus.*
✉ [3] *m.tsirlin@unitsky.com.*

ABSTRACT

The aerodynamic optimisation of the shape of a monorail suspended unibus of string transport has been described within the study on the influence of geometric and structural elements on aerodynamic characteristics. The estimate was carried out through a comparative analysis of the features of two shapes of a model with a further change and recalculation of the model being finalised. The comparison was focused on the drag force and the shape drag coefficient. The calculations used a gas dynamics model based on the Reynolds equations using the Menter SST-k-ω (shear stress transport) turbulence model. To solve the equations to find the design functions, an upwind second-order discretisation scheme was used applying the «pressure–velocity» refinement procedure in the framework of SIMPLE algorithm of Patankar–Spalding with the ANSYS Computational Fluid Dynamics Software. The dimensions of the computational domain were chosen considering the geometric dimensions of the 3D model of the shape. Boundary conditions were identified in the solver. The simulation was carried out for the case of motion of a vehicle at a constant speed.

The calculations have shown the importance and influence of the geometry of the transition sections of the vehicle body, the mandatory use of wheel fairings and the advantages of the S-shaped tail. The proposed design optimisation made it possible to reduce the drag force and coefficient by 16,9 %. The studies have resulted in selection of the optimal vehicle model which has the lowest aerodynamic drag coefficient, which made it possible to improve the energy efficiency of the system and its environmental friendliness, and consequently, the profit potential of the transportation process.

Keywords: string transport, unibus, aerodynamics, model, drag force, shape drag coefficient, pressure distribution on the frontal surfaces of the model, optimisation of the form shape.

For citation: Unitsky, A. E., Artyushevsky, S. V., Tsyrlin, M. I. Optimisation of the Aerodynamic Shape of a Monorail Suspended Unibus. World of Transport and Transportation, 2022, Vol. 20, Iss. 4 (101), pp. 163–172. DOI: https://doi.org/10.30932/1992-3252-2022-20-4-2.

The text of the article originally written in Russian is published in the first part of the issue.
Текст статьи на русском языке публикуется в первой части данного выпуска.

INTRODUCTION

Description of the Mathematical Model and Methods of Calculation of Aerodynamic Performance

The impact of the oncoming air flow with a speed V on the vehicle is reduced to loads continuously distributed over its surfaces. These distributed loads result in a net aerodynamic force applied at the centre of pressure and an aerodynamic moment around the centre of mass. The sum of drag and lift forces constitutes the aerodynamic force. The drag force itself is composed of pressure drag and friction drag [1].

When the air flows past the model, the oncoming air flow is compressed from the windward (frontal) side with formation of a high-pressure zone. The air flow, sliding across the contour, rushes to its rear part. The action of viscous friction forces causes an increase in the dynamic boundary layer and, subsequently, the air flow is separated from the surface and a trailing vortex is created behind it. In the rear part there is a zone of low pressure, where air inflow takes place constantly.

The pressure drag force is created due to the difference in air pressure on the frontal and rear parts of the vehicle. In turn, friction drag force is due to the attachment of layers of moving air to the surface of the model, because of which the air flow loses speed. In this case, the magnitude of the friction drag force depends on the properties of the material, quality, and condition of the surface [2].

The air flowing past a vehicle at a speed within the range of 150 km/h (41,7 m/s) occurs in a turbulent regime (Reynolds number Re = $13{,}5 \cdot 10^6 > 10^6$). In such cases, to solve practical problems of turbulent motion of flow, the system of Reynolds equations (RANS), continuity equations or analogues based on large-eddy methods, LES, are used:

$$\frac{\partial \overline{u_i}}{\partial x_i} = 0,\ \frac{\partial \overline{u_i}}{\partial t} + \frac{\partial \overline{u_j}\,\overline{u_i}}{\partial x_j} =$$

$$-\frac{1}{\rho}\frac{\partial \overline{p}}{\partial x_i} + \frac{\partial}{\partial x_i}\left[\nu\left(\frac{\partial \overline{u_i}}{\partial x_j} + \frac{\partial \overline{u_j}}{\partial x_i}\right) - \overline{u_i' u_j'}\right],$$

where $\overline{u_i'}$, $\overline{u_j'}$ – Reynolds stress closures based on the Boussinesq hypothesis with the help of the turbulent viscosity ν_t [3].

They are distinguished from the standard Navier–Stokes equations by the presence of an additional turbulent viscosity ν_t, which is many times greater than the molecular viscosity of the oncoming air.

According to [4], to solve external flow problems, it is recommended to use the Saffman–Wilcox k-ω model, the Spalart–Allmaras model, the Menter shear stress transport model, and the Launder and Jones k-ε model for the kinetic energy of turbulent fluctuations k and its dissipation rate ε.

For the numerical solution, a gas dynamics model based on the Reynolds equation (RANS approach) is used. In this formulation of the problem, the determined functions to be found are the velocity of air flowing past the surfaces of the unibus and the pressure on its surfaces; it is assumed that the air flow is isothermal and incompressible (constancy of temperature and density) as a medium flowing around the vehicle [5]. To solve the Reynolds equations, a turbulence model of the type of the Menter *SST-k-ω* shear stress transport model was chosen [6; 7].

Objective

The *objective* of this work was to provide information on aerodynamic optimisation of a monorail suspended unibus of complex geometric shape using the modern Computational Fluid Dynamics Simulation Software [8; 9].

RESULTS

Model Preparation and Procedure of the Study on the Aerodynamic Performance of the Model Shape

Constructing of a 3D model for computation was based on an assembly element of a monorail suspended unibus of string transport (Pic. 1); it was further refined considering the features of constructing a computational mesh: internal elements that do not affect aerodynamics were removed, external elements were merged into a single part, internal cavities were filled.

The dimensions of the computational domain were chosen considering the geometric dimensions of the 3D model. The calculation area is a parallelepiped with geometric dimensions of 50,0 x 11,5 x 13,0 m (Pic. 2).

For the calculation, a standard coordinate system is adopted: the direction of the *X*-axis is chosen opposite to the direction of movement of the vehicle, coincides with the direction of the drag force; *Y*-axis is a vertical upward axis that coincides with lift force; *Z*-axis is directed perpendicular to the *X*-axis in the horizontal plane.

Boundary conditions were identified in the solver of the ANSYS Fluent software [10]. The

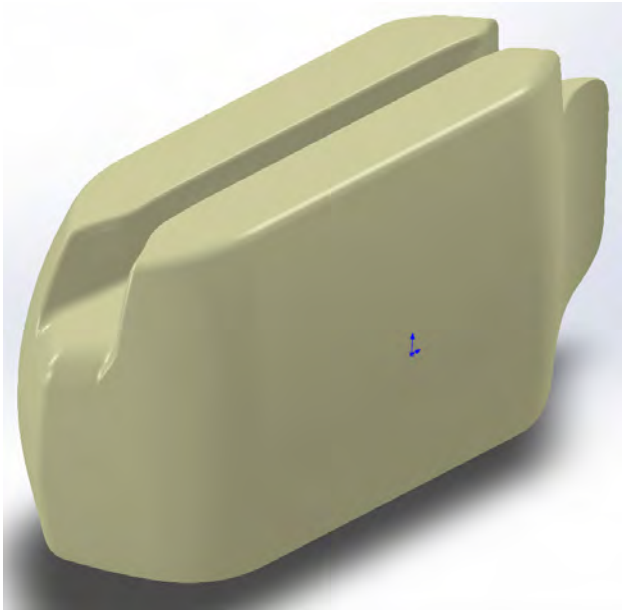

Pic. 1. Working 3D model of the shape of a monorail suspended unibus [developed by the authors].

simulation was performed for the case of motion at a constant speed, its longitudinal component was equal to the speed of the oncoming flow [11] and was set at the input boundary: speed of the oncoming flow was 41,7 m/s (150 km/h). Air flowing occurs at a normal atmospheric pressure of 101325 Pa and a constant temperature of 15°C, the turbulence intensity is 5 %, the turbulence scale is 10. «Soft» boundary conditions of the exit were taken at the output border. On the side surfaces of the computational domain, the wall conditions were set, but with zero friction (the condition of flow sliding near the wall), which made it possible to simulate the real conditions of an unlimited domain in a limited space [12]. For the surfaces of the model, sticking conditions were adopted (no slipping – No-slip).

The air at 20°C was chosen as a mobile (non-stationary) medium. The dimensions and type of the grid for all calculations are taken to be the same; preliminary analysis of the degree of mesh refinement showed a slight effect on the value of the sought-for drag coefficient. The

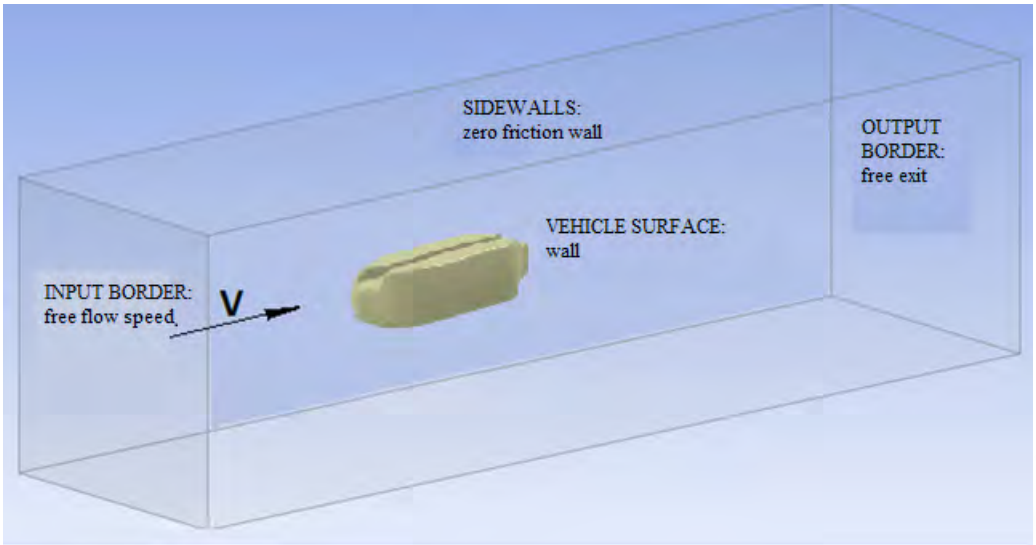

Pic. 2. Computational domain with a suspended unibus model [developed by the authors].

Pic. 3. Model No. 1 [developed by the authors].

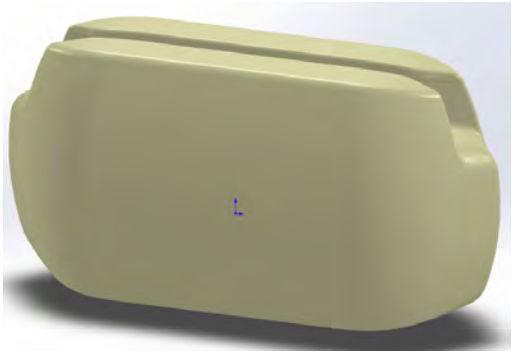

Pic. 4. Model No. 2 [developed by the authors].

maximum effect is determined when mesh was refined in the near-wall zone using a boundary layer with progressively changing dimensions of the first cell and adapting the mesh by splitting it two-fold. The calculation assumes an adaptation by the number $y+$ with a value of one. With $y+ = 1$, the mesh tends to a situation where several calculation nodes are formed in the near-wall layer. This allows considering the influence of the boundary layer. Each adaptation of the mesh refined the wall zone two-fold. Computation comprised 4 adaptations bringing $y+$ closer to one. After the fourth adaptation, the result is distorted, and further refinement becomes senseless. Hypothetically, this is due to a numerical error, since the size of the adaptive mesh changes by more than 20 % when halved, which leads to a distortion of the results obtained. As an assumption, the absence of the effect of compressibility of air is accepted. A significant manifestation of the compressibility effect appears when the Mach number is greater than 1/3, while the speed of sound in air under given conditions is close to 330 m/s, which is 2,6 times higher than the design speed of movement.

To solve the Reynolds equations with *SST-k-ω* Menter model to find the desired functions, the upstream second-order discretisation scheme was used using the «pressure–velocity» refinement procedure according to the SIMPLE Patankar–Spalding algorithm [13; 14].

Initialisation was carried out according to the flow parameters at the input border of the computational domain.

Assessment of Aerodynamic Performance

The assessment was carried out within a comparative analysis of the aerodynamic properties of two shapes with a further change and recalculation of the finalised model.

The following indicators were compared:

1. Pressure distribution field.
2. Force of frontal drag F_x.
3. Shape drag coefficient C_x.
4. Presence of turbulent flows.

Computation of drag force and coefficient was conducted in ANSYS Fluent software environment.

As it is known, the pressure field determines the aerodynamic wind resistance of any structure; the oncoming flow creates a high-pressure zone on the front surface; the maximum pressure corresponds to the point of greatest stagnation of the air flow.

The midsection in all models remained the same; the length varied in the range from 4,85 to 5,03 m.

The first pair of compared models determined the initial characteristics and showed the influence of the *S*-shaped tail fairing: in the first model, the «nose–tail» combination was used (Pic. 3), the second based on the «nose–nose» combination (Pic. 4).

Calculation results for the models No. 1 and No. 2 are shown in Table 1.

The result turned out to be the opposite to what was expected: the model No. 2, despite the absence of a *S*-shaped tail fairing, has got better aerodynamic performance.

After analysing and comparing the results of two calculations, a sharp drop in pressure on the side surface of model No. 1 became evident in the place where the radius of the rear fairing begins (Pic. 5). In the same place, model No. 2 shows only slight changes in pressure (Pic. 6).

Comparing the geometry of these elements, it should be noted (Pic. 7) that the desire to shorten the tail fairing of model No. 1, increasing the straight section of the cabin, leads to a decrease in the transition radius and to stall with deterioration in aerodynamic characteristics compared to model No. 2, despite its short fairing

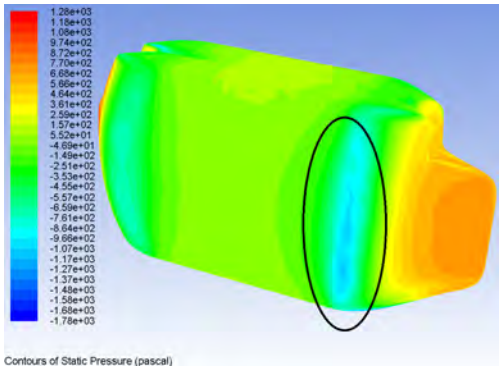

Pic. 5. Pressure distribution over the surface of the model No. 1 [developed by the authors].

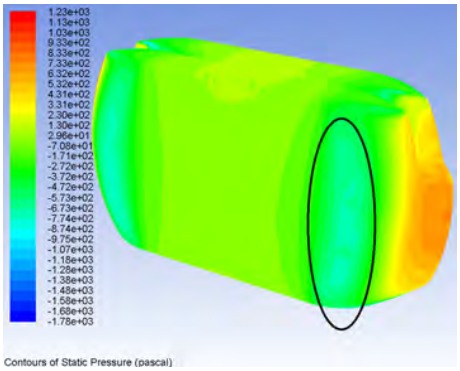

Pic. 6. Pressure distribution over the surface of the model No. 2 [developed by the authors].

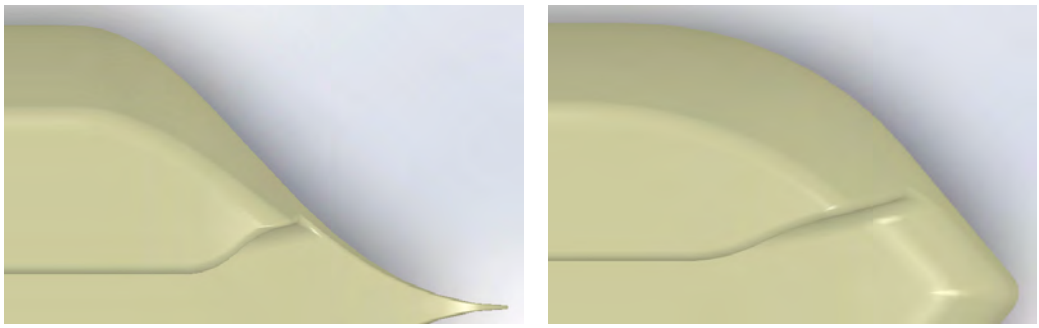

Pic. 7. Comparison of the configuration geometry of the models No. 1 and No. 2 [developed by the author].

Pic. 8. Change in the geometry of the tail fairing in the models No. 3 and No. 4 [developed by the authors].

Pic. 9. Model No. 3 [developed by the authors].

Pic. 10. Model No. 4 [developed by the authors].

Table 1 [compiled by the authors]

Model number	F_x, N	C_x
No. 1	330	0,095
No. 2	302	0,086

Table 2 [compiled by the authors]

Model number	F_x, N	C_x
No. 3	296	0,0845
No. 4	372	0,1065

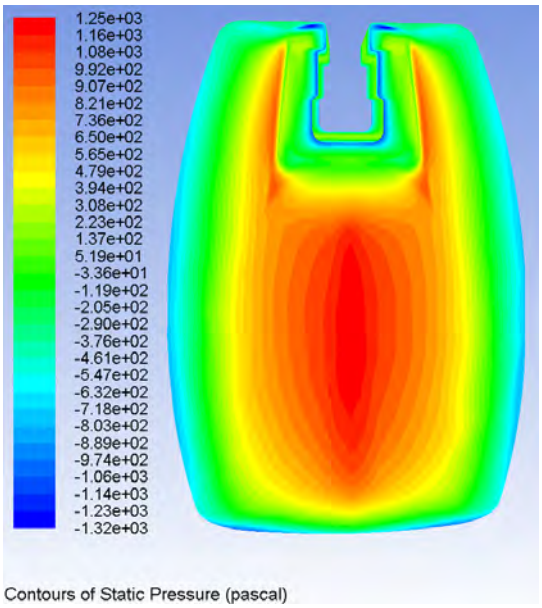

Pic. 11. Pressure distribution over the frontal surface of the model No. 3 [developed by the authors].

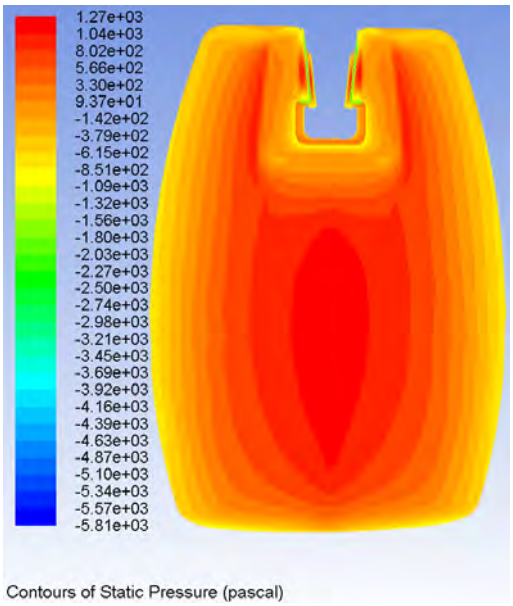

Pic. 12. Pressure distribution over the frontal surface of the model No. 4 [developed by the authors].

and the presence of bottom drag due to the «blunt» tail.

To improve the drag coefficient, it was recommended to increase the transition radius in the tail fairing of the next models.

The construction of models No. 3 and No. 4 considered the results of previous calculations; the transition radius in the tail fairing was increased (Pic. 8), also the effect of open and closed wheels was compared.

In model No. 3, the wheels are completely covered with fairings (Pic. 9), in model No. 4, the wheels protrude beyond the fairings (Pic. 10).

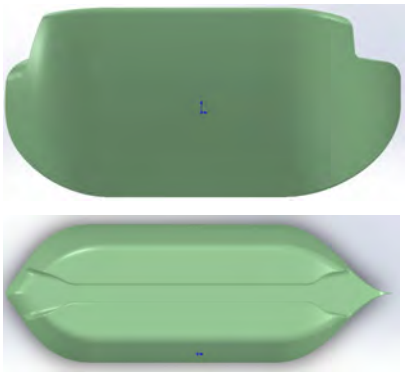

Pic. 13. Model No. 5 [developed by the authors].

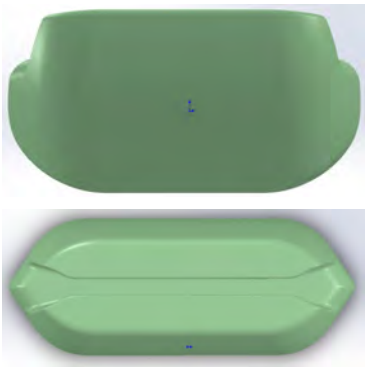

Pic. 14. Model No. 6 [developed by the authors].

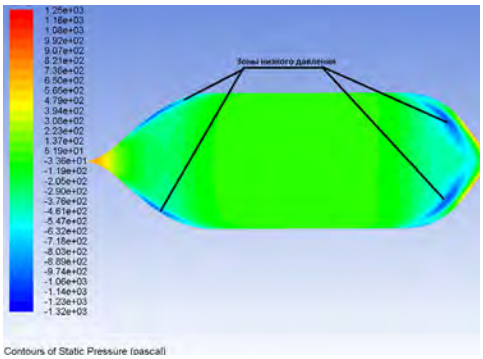

Pic. 15. Pressure distribution over the bottom of the vehicle of the model No. 3 [developed by the authors].

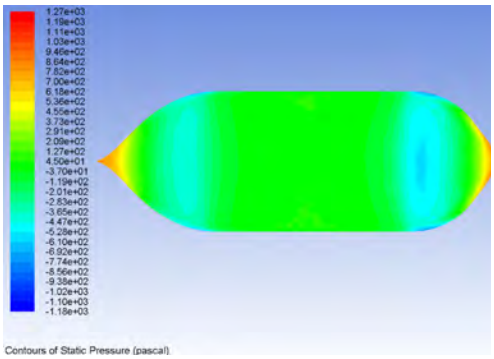

Pic. 16. Pressure distribution over the bottom of the vehicle of the model No. 5 [developed by the authors].

Calculation results for the models No. 3 and No. 4 are shown in Table 2.

The calculation showed a significant deterioration in the drag coefficient (by 26 %) with open wheels.

The frontal, lateral and tail surfaces of the models (Pics. 11, 12) are subject to the same pressure, while model No. 4 looks more «red» due to the drop in the lower pressure limit from -1,32e + 03 to -5,81e + 03, as a result of which the «green» zone has shifted up the scale; the difference is created by the rail tunnel and the wheels.

The conclusion is clear: the wheels must be covered with fairings.

Construction of models No. 5 and No. 6 considered the results of previous calculations: to improve aerodynamic features, the transition of the front and rear fairings to the bottom was changed (Pics. 13, 14), the effect of the *S*-shaped tail fairing was compared again.

Calculation results for the models No. 5 and No. 6 are shown in Table 3.

The calculation showed a positive effect of a smooth transition from the nose and tail fairings to the bottom; due to the absence of a sharp transition, the low-pressure zones, that had caused flow stall and induced air turbulence, practically disappeared (Pics. 15, 16).

In the frontal part, the high-pressure zone decreased (Pic. 17), reducing the component of the pressure drag force. It should be noted that a decrease in the lower pressure limit also has a positive effect on the aerodynamic characteristics.

The pressure distribution in the tail section is almost the same, except for the bottom drag in model No. 6, due to the «blunt tail» and the intersection of two flows from the side surfaces.

Table 3 [compiled by the authors]

Model number	F_x, N	C_x
No. 5	273	0,0780
No. 6	278	0,0795

Table 4 [compiled by the authors]

Model number	F_x, N	C_x
No. 7	274	0,0782
No. 8	272	0,0778

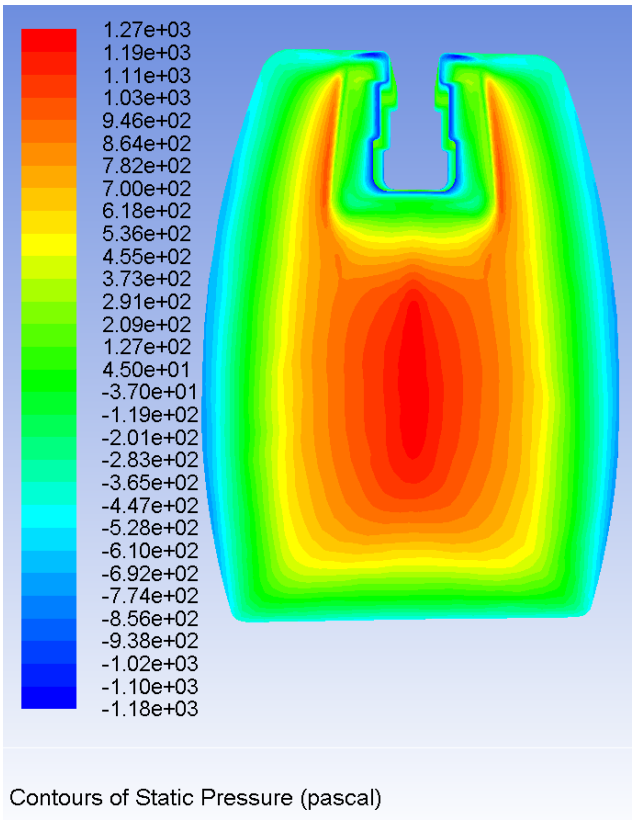

Pic. 17. Pressure distribution on the frontal surface of the models No. 5 and No. 6 [developed by the authors].

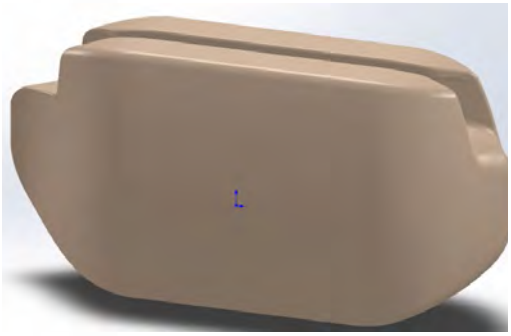

Pic. 18. Model No. 7 [developed by the author]).

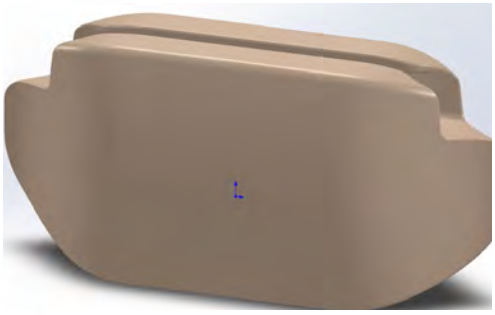

Pic. 19. Model No. 8 [developed by the authors].

In model No. 5, due to the *S*-shaped tail fairing, the flows do not intersect, but exit in parallel. That, considering the symmetry of the model, creates co-directional air flows moving at the same speed, these techniques reduce, and in some places completely eliminate the formation of Karman vortex streets.

The model No. 7 is the Model No. 5 rotated 180° (Pic. 18) (determination of aerodynamic characteristics when reversing); in model No. 8, the «tail–tail» combination was used (Pic. 19).

Calculation results for the models No. 7 and No. 8 are given in Table 4.

Calculations showed that the increase in the drag force when reversing at these speeds was 0,25 %; it can be said that vehicles with the shape implemented in models No. 5 and No. 7 are able to move forward / backward with the same aerodynamic characteristics at speeds $V = 41{,}7$ m/s.

The calculation of model No. 8 showed a slight improvement in aerodynamic characteristics (by the same 0,25 %), therefore, in the following calculations, considering crosswinds, the shapes that showed the best results, namely, models No. 5 and No. 8, were compared.

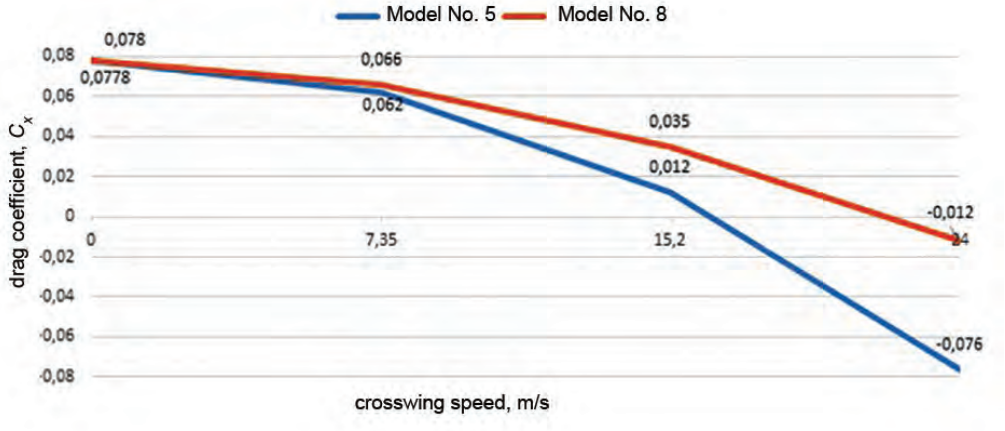

Pic. 20. Dependences of the drag coefficient C_x on the crosswind speed [developed by the authors].

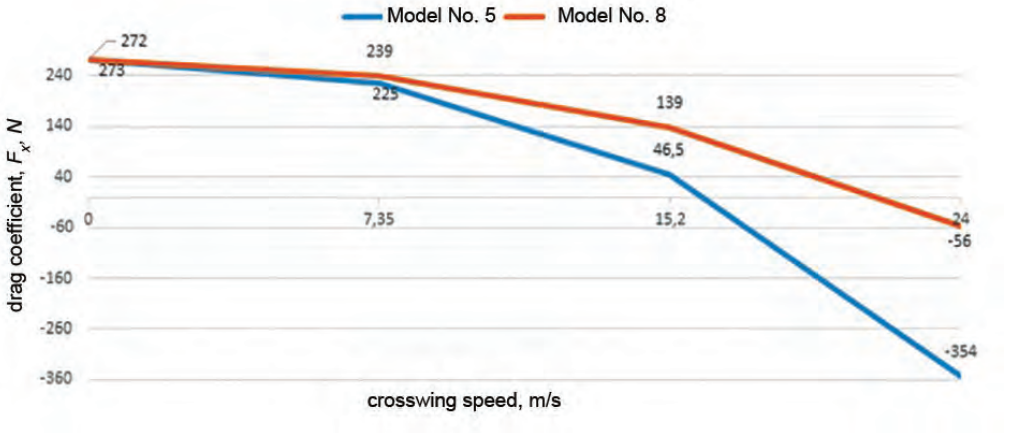

Pic. 21. Dependences of the resistance force F_x on the crosswind speed [developed by the authors].

To determine the characteristics, considering the impact of the crosswind, the calculated zone of wind-tunnel testing was rotated relative to the vehicle and the coordinate system at an angle of respectively 10, 20 and 30 degrees, which corresponded to a crosswind speed of 7,35; 15,2 and 24 m/s, respectively. The speed of the oncoming flow as a resultant value took the values V_{10} = 42,34 m/s, V_{20} = 44,37 m/s and V_{30} = 48,15 m/s.

As a separate characteristic necessary to determine the wind loads on the track structure, the drag force and coefficient of the shape of a stationary vehicle from the wind directed at an angle of 90° with a speed of V_{90} = 24 m/s were determined.

The calculation results for the models No. 5 and No. 8 are shown in Table 5 and graphically in Pics. 20 and 21.

As the calculation results showed, model No. 5, due to the rounded front fairing, has better characteristics, despite the higher coefficient and drag force at zero crosswind speed. Model No. 8

Table 5 [compiled by the authors]

Model number	Wind speed 7,35 m/s, vehicle speed 41,7 m/s		Wind speed 15,2 m/s, vehicle speed 41,7 m/s		Wind speed 24 m/s, vehicle speed 41,7 m/s		Wind speed 24 m/s, vehicle speed 0 m/s	
	F_{x10}, N	C_{x10}	F_{x20}, N	C_{x20}	F_{x30}, N	C_{x30}	F_{90}, N	C_{x90}
No. 5	225	0,062	46,5	0,012	-354	-0,076	2229	0,652
No. 8	239	0,066	139	0,035	-56	-0,012	2430	0,699

has a flat spade-shaped nose, which under a crosswind becomes a kind of sail, worsening the flow of the oncoming air, and increasing the impact of wind load on the track [monorail] structure.

Negative values of the drag coefficient C_x and force F_x for vehicle at rest are associated with the change in the difference between the zones of high and low pressure in the front and rear zones in the adopted coordinate system, with the geometric features of the shape of the vehicles, as can be seen from the smaller influence regarding the symmetrical model No. 8.

CONCLUSIONS

The study referred to consequent optimisation of the complex geometric shape of the body of a monorail string vehicle, that was a unibus. The calculations showed the importance and influence of the geometry of the body transition sections, the mandatory use of wheel fairings and the advantages of the *S*-shaped tail fairing. All these factors to varying extents affect the value of the total aerodynamic resistance to motion of a vehicle. Therewith, the proposed design optimisation makes it possible to reduce the force and drag coefficient by 16,9 %. Based on the results of the research, the optimal vehicle model was selected, which has the lowest aerodynamic drag coefficient, allowing to improve the energy efficiency of the system and environmental friendliness, and, consequently, the profit potential of the transportation process.

REFERENCES

1. Mkhitaryan, A. M. Aerodynamics [*Aerodinamika*]. Moscow, Ekolit publ., 2013, 448 p. ISBN 978-5-4365-0050-8.

2. Kvasnovskaya, N. P., Kvasnovsky, A. S. Aerodynamics of modern passenger cars [*Aerodinamika sovremennykh legkovykh avtomobilei*]. *Avtotransportnoe predpriyatie,* 2006, Iss. 3, pp. 51−55.

3. Wilcox, D. C. Turbulence modeling for CFD. 3rd ed. DCW industries, 2006, Vol. 2, 522 p. ISBN 978-1-928729-08-2 (1-928729-08-8).

4. Belov, I. A., Isaev, S. A. Modelling of turbulent flows: Study guide [*Modelirovanie turbulentnykh techenii: Ucheb. posobie*]. St. Petersburg, Baltic State Technical University, 2001, 108 p.

5. Molchanov, A. M. Thermophysics and Dynamics of Fluid and Gas [*Termofizika i dinamika zhidkosti i gaza*]. Moscow, MAI publ., 2019, 152 p. [Electronic resource]: https://k204.ru/downloads/text2019.pdf. Last accessed 24.05.2022.

6. Menter, F. R., Kuntz, M., Langtry, R. Ten Years of Industrial Experience with the SST Turbulence Model. *Turbulence, heat and mass transfer*, 2003, Vol. 4, No. 1, pp. 625−632. [Electronic resource]: https://www.researchgate.net/publication/228742295_Ten_years_of_industrial_experience_with_the_SST_turbulence_model. Last accessed 24.05.2022.

7. Snegirev, A. Yu. High performance computing in technical physics. Numerical modelling of turbulent flows: Study guide [*Vysokoproizvoditelnie vychisleniya v tekhnicheskoifizike. Chislennoe modelirovanie turbulentnykh techenii: Ucheb. posobie*]. St. Petersburg, SPU publ., 2009, 143 p. ISBN 978-5-7422-2317-7.

8. Unitsky, A. E. String transport systems: on Earth and in space [*Strunnie transportnie sistemy: na Zemle i v Kosmose*]. Silakrogs, PNB print, 2019, 576 p. ISBN 978-985-90498-1-1.

9. Unitsky, A. E., Garakh, V. A., Tsyrlin, M. I. String transport for urban transportation of passengers [*Strunniy transport dlya gorodskikh perevozok passazhirov*]. *Nauka i tekhnika transporta*, 2021, Iss. 3, pp. 19–25. DOI: 10.53883/ 20749325_2021_03_19.

10. Pastukhov, D. F., Volosova, N. K., Pastukhov, Yu. F. Construction of non-stationary models in the ANSYS FLUENT shell: Study guide [*Postroenie nestatsionarnykh modelei v obolochke ANSYS FLUENT: Ucheb. posobie*]. Novopolotsk, PSU publ., 2018, 46 p. [Electronic resource]: https://elib.psu.by/bitstream/ 123456789/22092/3/Построение%20нестационарных%20моделей%20в%20оболочке%20Fluent%20WORKBENCH.pdf. Last accessed 24.05.2022.

11. Andreichyk, A. F., Shmeliov, A. V., Kharytonchyk, S. V. The estimated assessment of aerodynamic losses into the trailer-trailer gap of the linked road vehicle. *Aktualnie voprosy mashinovedeniya*, 2015, Iss. 4, pp. 121−124. [Electronic resource]: https://elibrary.ru/item.asp?id=29305331. Last accessed 24.05.2022.

12. Vysotsky, M. S., Evgrafov, A. N. Aerodynamics of wheel transport [*Aerodinamika kolesnogo transporta*]. Minsk, Belavtotraktorstroenie publ., 2001, 363 p. ISBN 985-6637-03-1.

13. Patankar, S. V., Spalding, D. B. Heat and Mass Transfer in Boundary Layers. Transl. from English [*Russian title: Teplo- I massobmen v pogranichnykh sloyakh*]. Moscow, Energia publ., 1971, 128 p.

14. Minkov, L. L., Moiseeva, K. M. Numerical solution of hydrodynamic problems using the Ansys Fluent computer package [*Chislennoe rechenie zadach gidrodinamiki s pomoshchyu vychislitelnogo paketa Ansys Fluent*]. Tomsk, STT, 2017, 122 p. ISBN 978-5-93629-594-2. [Electronic resource]: https://elibrary.ru/item.asp?id=29806159. Last accessed 24.05.2022. ●

Information about the authors:

Unitsky, Anatoli E., *Chairman of the Board of Directors, General Designer of CJSC String Technologies, Minsk, Belarus, a@unitsky.com.*

Artyushevsky, Sergey V., *Deputy General Designer for Research of CJSC String Technologies, Minsk, Belarus, s.artyushevskiy@unitsky.com.*

Tsyrlin, Mikhail I., *Ph.D. (Eng), Leading Specialist of the Research Department of CJSC String Technologies, Minsk, Belarus, m.tsirlin@unitsky.com.*

Article received 04.04.2022, approved 06.09.2022, accepted 10.09.2022.